1521-0111/12/8202-209–216$25.00
MOLECULAR PHARMACOLOGY
Copyright © 2012 The American Society for Pharmacology and Experimental Therapeutics
Mol Pharmacol 82:209–216, 2012

Vol. 82, No. 2
78642/3781651

Augmentation of Reduced Folate Carrier-Mediated Folate/Antifolate Transport through an Antiport Mechanism with 5-Aminoimidazole-4-Carboxamide Riboside Monophosphate

Michele Visentin, Rongbao Zhao, and I. David Goldman

Departments of Medicine and Molecular Pharmacology, Albert Einstein College of Medicine, Bronx, New York

Received March 7, 2012; accepted May 3, 2012

ABSTRACT

5-Aminoimidazole-4-carboxamide riboside (AICAR), an agent with diverse pharmacological properties, augments transport of folates and antifolates. This report further characterizes this phenomenon and defines the mechanism by which it occurs. Exposure of HeLa cells to AICAR resulted in augmentation of methotrexate, 5-formyltetrahydrofolate, and 5-methyltetrahydrofolate initial rates and net uptake in cells that express the reduced folate carrier (RFC). This did not occur in cells that express only the proton-coupled folate transporter and accumulated folates by this mechanism. Transport stimulation correlated with the accumulation of 5-aminoimidazole-4-carboxamide ribotide monophosphate (ZMP), the monophosphate derivative of AICAR, within cells as established by liquid chromatography. When ZMP formation was blocked with 5-iodotubercidin, an inhibitor of adenosine kinase, folate transport stimulation by AICAR was absent. When cells first accumulated ZMP and were then exposed to 5-iodotubercidin or AICAR-free buffer, the ZMP level markedly decreased and folate transport stimulation was abolished. Extracellular ZMP inhibited RFC-mediated folate influx, and the presence of intracellular ZMP correlated with inhibition of folate efflux. The data indicate that intracellular ZMP trans-stimulates folate influx and inhibits folate efflux, which, together, produce a marked augmentation in the net cellular folate level. This interaction among ZMP, folates, and RFC, a folate/organic phosphate antiporter, is consistent with a classic exchange reaction. The transmembrane gradient for one transport substrate (ZMP) drives the uphill transport of another (folate) via a carrier used by both substrates, a phenomenon intrinsic to the energetics of RFC-mediated folate transport.

Introduction

The mechanisms of membrane transport of the B_9 folate vitamins has been a topic of considerable interest (Kamen and Smith, 2004; Assaraf, 2006; Matherly and Hou, 2008; Zhao et al., 2009, 2011). Folate sufficiency in humans requires efficient intestinal absorption and transport of folates into systemic tissues. Antifolates currently in clinical use, methotrexate, pemetrexed, and pralatrexate, are all highly hydrophilic and require carrier-mediated transport into tumor cells to achieve their anticancer activities (Goldman et al., 2010). Folates are transported by three genetically distinct folate-specific mechanisms used to different extents by antifolate agents. Folates are absorbed in the proximal jejunum by the proton-coupled folate transporter (PCFT) (SLC46A1), which is also widely expressed in epithelial cancers (Qiu et al., 2006), and are transported into systemic tissues primarily by the reduced folate carrier (RFC) (SLC19A1), an organic phosphate antiporter (Kamen and Smith, 2004; Assaraf, 2006; Matherly and Hou, 2008; Zhao et al., 2009, 2011). Folates are also transported via receptor-mediated endocytosis. Folate receptor-α is expressed predominantly at the epithelial membrane of several tissues and in a broad spectrum of epithelial cancer cells (Kamen and Smith, 2004; Assaraf, 2006; Matherly and Hou, 2008; Zhao et al., 2009, 2011). These concentrative processes are opposed by the ATP-binding cassette exporters, the multidrug resistance-associated proteins, and the breast cancer resistance protein, ubiquitously expressed in human cells, that pump

This work was supported by the National Institutes of Health National Cancer Institute [Grant CA82621].
Article, publication date, and citation information can be found at http://molpharm.aspetjournals.org.
http://dx.doi.org/10.1124/mol.112.078642.

ABBREVIATIONS: PCFT, proton-coupled folate transporter; RFC, reduced folate carrier; AICAR, 5-aminoimidazole-4-carboxamide riboside; MTX, methotrexate; ZMP, 5-aminoimidazole-4-carboxamide ribotide monophosphate; 5-formyl-THF, (6*S*)5-formyltetrahydrofolate; 5-methyl-THF, (6*S*)5-methyltetrahydrofolate; HPLC, high-performance liquid chromatography; DHFR, dihydrofolate reductase; ZDP, 5-aminoimidazole-4-carboxamide ribotide diphosphate; ZTP, 5-aminoimidazole-4-carboxamide ribotide triphosphate; mTOR, mammalian target of rapamycin.

folates unidirectionally out of cells (Kamen and Smith, 2004; Assaraf, 2006; Matherly and Hou, 2008; Zhao et al., 2009, 2011).

5-Aminoimidazole-4-carboxamide riboside (AICAR) was shown to enhance MTX and 5-formyltetrahydrofolate uptake into CCRF-CEM T leukemia cells (McGuire et al., 2006). This effect was attributed to the salutary impact of AICAR on RFC function (McGuire et al., 2006). However, the mechanism by which this occurred was not established nor was the possibility that the enhanced net transport of folates might be a result of inhibition of ATP-binding cassette exporters excluded. The current study explores this phenomenon further in unique HeLa cell lines, developed in this laboratory, that express either RFC or PCFT to establish the role of each transporter in this phenomenon. Cells that express only PCFT also allow the accumulation of folates in the absence of RFC to clarify the potential impact of AICAR on the ATP-binding cassette exporters that influence net transport of folates within cells. These studies establish that AICAR potentiation of folate transport is, in fact, RFC-mediated and that this is due to the buildup of the 5′-monophosphate derivative of AICAR, ZMP, with cells. ZMP participates in an exchange reaction with folates that results in the trans-stimulation of folate influx and the suppression of folate efflux that together enhance net accumulation of folates and MTX within these cells.

Materials and Methods

Reagents. Tritiated (6*S*)5-formyltetrahydrofolate (5-formyl-THF), (6*S*)5-methyltetrahydrofolate (5-methyl-THF), MTX, and AICAR were obtained from Moravek Biochemicals (Brea, CA) with purity established and monitored by high-performance liquid chromatography (HPLC) as described previously (Zhao et al., 2000). Nonlabeled 5-formyl-THF and 5-methyl-THF were purchased from Schircks Laboratories (Jona, Switzerland). MTX was obtained from Sigma-Aldrich (St. Louis, MO), AICAR was purchased from Cayman Chemical (Ann Arbor, MI), and ZMP was from Sigma-Aldrich. 5-Iodotubercidin was obtained from Tocris Bioscience (Bristol, UK).

Cell Lines. Cells were maintained in RPMI 1640 medium supplemented with 10% fetal bovine serum (Gemini Bio-Products, Irvine, CA), 100 units/ml penicillin, and 100 μg/ml streptomycin at 37°C in a humidified atmosphere of 5% CO_2. HeLa R1-PCFT cells and HeLa R1-RFC6 cells, which express only PCFT or RFC, respectively, were derived from HeLa R1–11 cells and were maintained in 300 μg/ml hygromycin B (Calbiochem, San Diego, CA) and 100 μg/ml phleomycin (Zeocin; Invitrogen, Carlsbad, CA), as reported previously (Zhao et al., 2004b, 2008; Diop-Bove et al., 2009).

Transport Measurement. Transport of tritiated substrates was measured in cells grown in monolayer culture at the bottom of glass vials for 3 days (Sharif and Goldman, 2000). The medium was aspirated, 1 ml of HBS buffer (20 mM HEPES, 140 mM NaCl, 5 mM KCl, 2 mM $MgCl_2$, and 5 mM dextrose; adjusted with 1 N NaOH to achieve a pH of 7.4) was added, and the vials were incubated in a 37°C water bath for 20 min. AICAR was added to achieve the indicated concentrations and, after incubation for the indicated times, buffer was aspirated, and radiolabeled substrate was added. Uptake was stopped by injection of 10 volumes of ice-cold HBS buffer at pH 7.4 after which the cells were washed three times in this buffer and then were digested with 0.2 N NaOH at 65°C for 45 min. Specimens were taken for assessment of intracellular tritium on a liquid scintillation spectrometer (400 μl) or protein (10 μl) by the BCA assay (Thermo Fisher Scientific, Waltham, MA). Intracellular radioactivity is expressed as picomoles of tritiated substrate per milligram of protein. Influx kinetics were determined by a nonlinear regression analysis of the relationship between MTX influx and the extracellular MTX concentration based on the Michaelis-Menten equation using Prism (version 5.0 for Windows; GraphPad Software Inc., San Diego, CA).

For efflux measurements, cells were incubated with [^{3}H]MTX in transport buffer in the presence or absence of AICAR after which 5-formyl-THF was added to achieve an extracellular concentration of 100 μM to completely block influx. Then the declining level of intracellular MTX, which reflects the unidirectional efflux of this agent, was monitored. Samples were processed for radioactivity and protein as indicated above. Free intracellular MTX could be discriminated from total drug by assessing the component bound to dihydrofolate reductase (DHFR) 30 to 60 min after cells loaded with [^{3}H]MTX were washed and then exposed to a large volume of drug-free medium (Zhao et al., 2004a).

HPLC of [^{3}H]AICAR and Its Metabolites. After incubation with 1 mM [^{3}H]AICAR, cells were washed twice in ice-cold HBS. An acid-soluble extract of cells was obtained by addition of ice-cold 5% trichloroacetic acid after which the acid-insoluble and -soluble fractions were separated by centrifugation at 4000*g* for 10 min. The acid-insoluble fraction was digested in 2 ml of 0.2 N NaOH at 65°C, and a portion was taken for protein determination as indicated above. The acid-soluble fraction was extracted twice with diethyl ether and then was passed through a 45-μm filter and stored at −80°C. Analyses were performed on a Beckman System Gold high-performance liquid chromatograph. Samples were applied to a 4.6 × 250 mm ion-exchange column (Phenomenex, Torrance, CA) and eluted with a linear gradient of 5 mM $NH_4H_2PO_4$, pH 2.8, to 750 mM $NH_4H_2PO_4$, pH 3.9, over 25 min at a flow rate of 0.8 ml/min. Absorbance was monitored at 280 nm. The eluted fractions were collected, and radioactivity was determined. Intracellular ZMP concentration was determined from the difference between the wet and the dry weights of a cell pellet less the inulin space as reported previously (Zhao et al., 1997).

Statistical Analysis. Statistical comparisons were performed with the two-tailed Student's paired *t* test. All statistical analyses were performed with GraphPad Prism.

Results

Impact of AICAR on Folate and Antifolate Influx and Net Accumulation in HeLa Cells. After a 10-min incubation with 1 mM AICAR, tritiated MTX, 5-formyl-THF, or 5-methyl-THF was added to achieve a concentration of 0.5 μM and uptake assessed in HeLa cells. It can be seen in Fig. 1, top, that the uptake slopes over the first 5 min were linear and extrapolate through the point of origin, reflecting the unidirectional flux of these substrates into these cells. Initial uptake rates were enhanced 2- to 4-fold by AICAR. As indicated in Fig. 1, bottom, net uptake of all three substrates was markedly increased in AICAR-treated cells. For MTX, a steady state was achieved that was ~3-fold greater in cells exposed to AICAR than in control cells. However, the augmented uptake of free drug was considerably higher when the component tightly bound to dihydrofolate reductase, indicated by the interrupted line, was considered. When cells were incubated with 1 mM AICAR simultaneously with MTX, stimulation of uptake emerged over 5 to 10 min (not shown). Hence, stimulation was not instantaneous and, as later shown, was dependent upon uptake and metabolism of AICAR within the cells.

Distinguishing among the Roles of RFC, PCFT, and ATP-Binding Cassette Exporters in AICAR Potentiation of MTX and 5-Formyl-THF Transport. Because HeLa cells express both RFC and PCFT, studies were under-

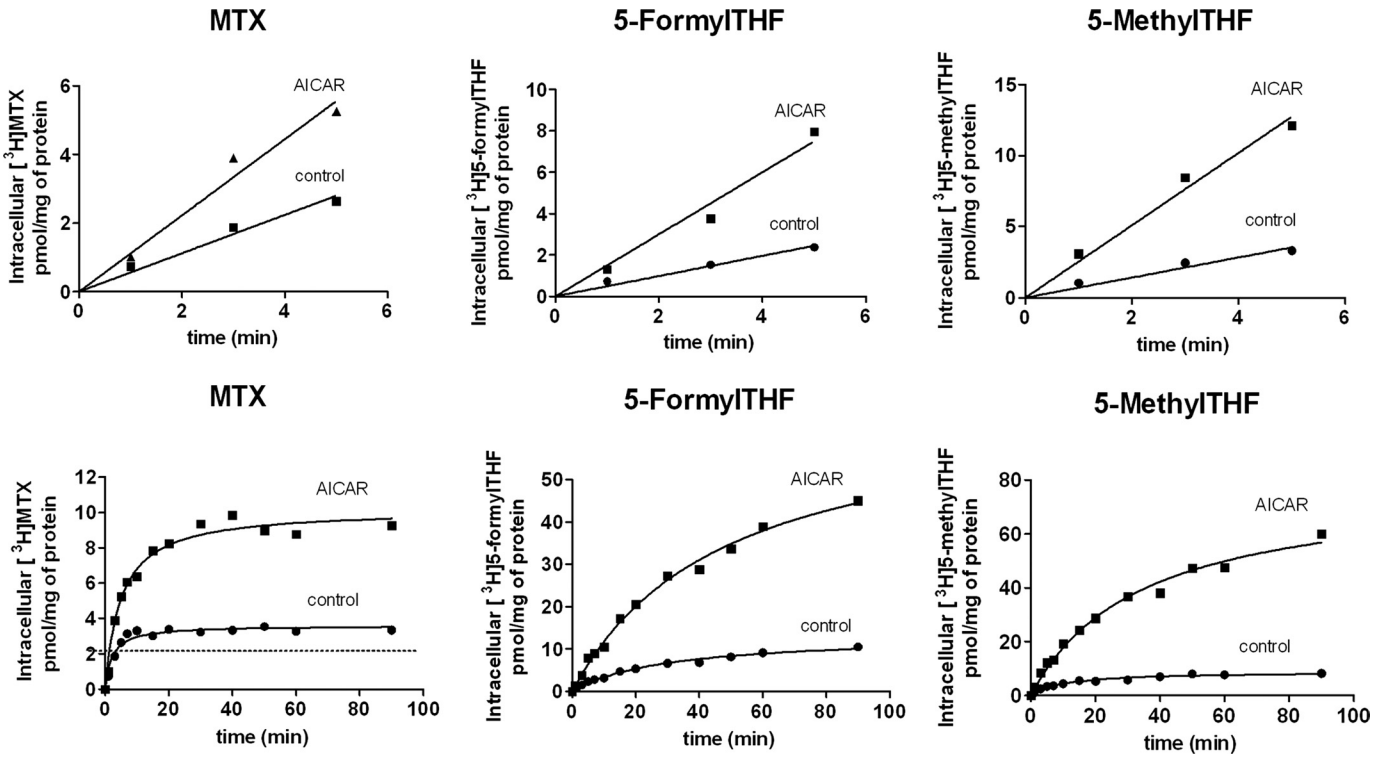

Fig. 1. Impact of 1 mM AICAR on folate influx and net uptake in HeLa cells. Transport of 0.5 μM [^{3}H]MTX (left), [^{3}H]5-formyl-THF (center), and [^{3}H]5-methyl-THF (right) in the presence and absence of 1 mM AICAR. AICAR was added 10 min before addition of folates and was present during the transport measurements. Top, initial rates of folate uptake (influx). Bottom, the time course of the net uptake of folates. The horizontal interrupted line in bottom left represents MTX tightly bound to dihydrofolate reductase. The different between bound and total intracellular MTX is the component free within the intracellular water (see *Materials and Methods*). The data are from an experiment representative of three independent experiments.

taken to explore the potential role of each of these transporters in this phenomenon using HeLa R1–11 cells, which lack endogenous folate transporters, stably transfected with either RFC (HeLa R1-RFC6 cells) or PCFT (HeLa R1-PCFT). When PCFT was the carrier by which cells were loaded with folates, it was possible to determine the extent to which AICAR affects the activity of this transporter as well as that of other transporters that act on the disposition of intracellular folates and could have an impact on their accumulation in cells. For instance, the stimulatory effect of AICAR on net folate uptake could be due to inhibition of ATP-binding cassette exporters that pump folates out of cells, resulting in enhanced influx and uphill folate transport. It can be seen that net uptakes of tritiated MTX (Fig. 2, top left panel) and 5-formyl-THF (Fig. 2, top right) were both enhanced by AICAR in cells that express only RFC. However, as indicated

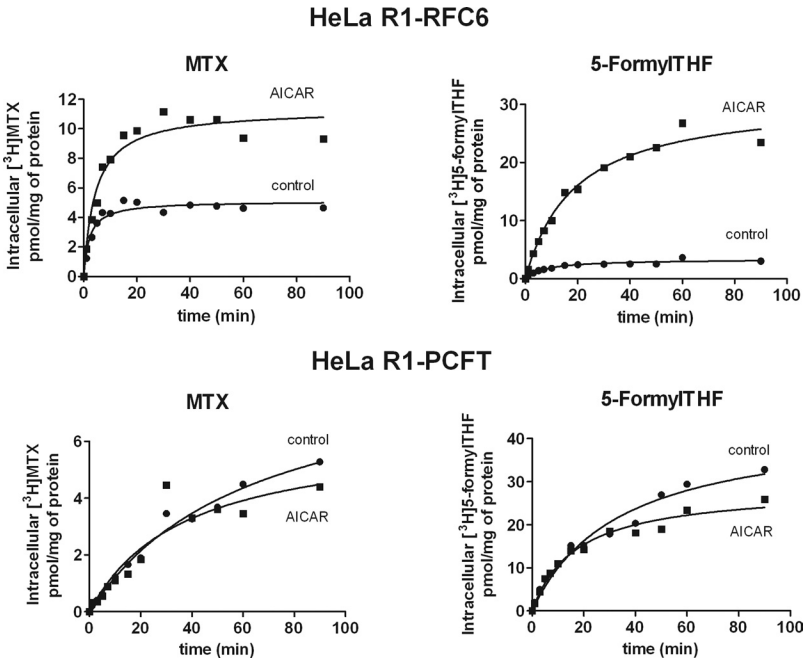

Fig. 2. Roles of RFC and PCFT in AICAR potentiation of net folate transport. Top, net uptake of 0.5 μM [^{3}H]MTX (left) and [^{3}H]5-formyl-THF (right) in the presence and absence of 1 mM AICAR in cells that express only RFC (HeLa-RFC6). Bottom, net uptake of 0.5 μM [^{3}H]MTX (left) and [^{3}H]5-formyl-THF (right) in the presence and absence of 1 mM AICAR in cells that express only PCFT (HeLa-PCFT). AICAR was added 10 min before addition of folates and was present during the transport measurements. The data are representative of three independent experiments.

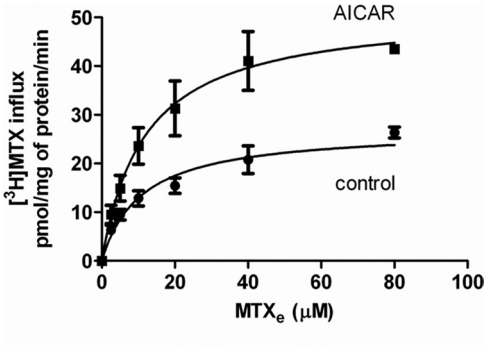

	control	AICAR
K_t	11.0 ± 2.7	11.9 ± 3.5
V_{max}	27.1± 2.3	51.4 ± 5.5

Fig. 3. Impact of AICAR on RFC influx kinetics. HeLa cells were incubated in the presence or absence of 1 mM AICAR for 10 min after which influx of [^{3}H]MTX was assessed in the presence of this agent. The line is best fit to the Michaelis-Menten equation ($V = V_{max}[S]/(K_t+[S])$. K_t is in micromoles per liter and represents the extracellular concentration (MTX_e) at which MTX influx is half of maximum; V_{max} is in picomoles per milligram of protein per minute. Results are the mean ± S.E.M. from three independent experiments.

in Fig. 2, bottom, this did not occur in the cells that express only PCFT; indeed, there was a small decrease in net uptake late in the uptake process. This experimental design excludes a role for PCFT in the AICAR effect or AICAR-induced suppression of ATP cassette proteins that export folates from cells. Because PCFT is not involved in the augmentation of transport by AICAR, and studies are performed at pH 7.4 when PCFT-mediated MTX transport is negligible, subsequent experiments could be performed with wild-type HeLa cells.

Impact of AICAR on MTX Influx Kinetics Mediated by RFC. The kinetic basis for the augmentation of RFC-mediated MTX influx by AICAR in HeLa cells is indicated in Fig. 3. On the basis of a nonlinear regression analysis of influx as a function of the extracellular MTX concentration, the influx K_t was unchanged; rather, the sole alteration was an ~2-fold increase in the influx V_{max} from 27.1 ± 2.3 to 51.4 ± 5.5 pmol · mg protein^{-1} · min^{-1}. Hence, treatment of cells with AICAR results in an increase in the rate-limiting step in the RFC transport cycle.

Reversibility of the Augmentation of RFC-Mediated Transport by AICAR. To assess the reversibility of the AICAR effect, cells exposed to 1 mM AICAR for 10 min were washed in 0°C AICAR-free buffer and then were exposed to this buffer for 30 min after which transport of [^{3}H]5-formyl-THF was assessed. As indicated in Fig. 4A, the stimulation of influx (inset) and net transport was completely reversed. Figure 4B illustrates the time course of the reversal. Cells exposed to 1 mM AICAR for 10 min were washed in 0°C AICAR-free buffer then exposed to this buffer at 37°C at time 0. It can be seen that influx stimulation was sustained for 3 to 4 min (inset) after which the rate of uptake declined to the level observed in control cells not exposed to AICAR. Ultimately, the same steady-state level was reached in the AICAR-exposed and control cells. Hence, AICAR-induced stimulation of folate transport is rapidly reversible.

Impact of 5-Iodotubercidin on AICAR Metabolism and Stimulation of RFC-Mediated Transport. The observation that AICAR potentiation of RFC-mediated transport was not instantaneous suggested that AICAR transport into cells, followed by its conversion to a phosphorylated derivative, might be a prerequisite for this phenomenon. The first step in AICAR metabolism is its phosphorylation to ZMP mediated by adenosine kinase. When cells were exposed to a 1 μM concentration of the potent (IC_{50} = 25 nM) adenosine

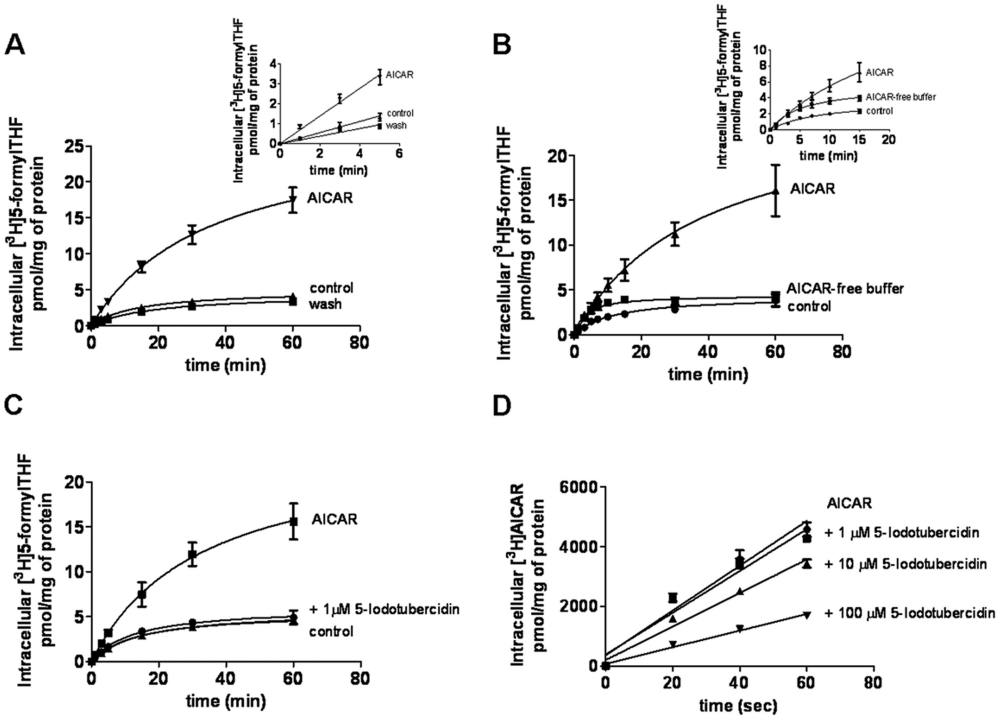

Fig. 4. The impact of 5-iodotubercidin and the reversibility of AICAR stimulation of RFC-mediated transport. A, cells were preincubated for 10 min with 1 mM AICAR and then were incubated for 30 min in AICAR-free buffer after which uptake of 0.5 μM [^{3}H]5-formyl-THF was assessed. Results are the mean ± S.E.M. from three independent experiments. The inset amplifies the initial uptake over 5 min. B, cells were preincubated for 10 min with 1 mM AICAR and then were exposed to AICAR-free buffer at time 0, and uptake of [^{3}H]5-formyl-THF was assessed. The inset amplifies uptake over the first 15 min. Results are the mean ± S.E.M. from three independent experiments. C, time course of uptake of 0.5 μM [^{3}H]5-formyl-THF in HeLa cells preincubated for 10 min with 1 mM AICAR in the presence and absence (control) of 1 μM 5-iodotubercidin. Data are the mean ± S.E.M. from three independent experiments. D, initial rate of 1 mM [^{3}H]AICAR uptake in HeLa cells as a function of 5-iodotubercidin concentration. Data are the mean ± S.E.M. from three independent experiments.

kinase inhibitor, 5-iodotubercidin (Parkinson and Geiger, 1996), the stimulation of RFC-mediated uptake of 0.5 μM [^{3}H]5-formyl-THF uptake by AICAR was abolished (Fig. 4C). Because 5-iodotubercidin is a nucleoside analog and can inhibit nucleoside transporters (Parkinson and Geiger, 1996), it was necessary to exclude the possibility that its inhibitory effects were related to inhibition of AICAR transport. However, as indicated in Fig. 4D, 1 μM 5-iodotubercidin had no effect on influx of [^{3}H]AICAR, confirming that its inhibitory effect, at this concentration, was due solely to its suppression of AICAR metabolism. The inhibition observed at higher concentrations of 5-iodotubercidin is consistent with transport of AICAR via a facilitated process (Gadalla et al., 2004).

The basis for these effects of 5-iodotubercidin was confirmed by an analysis of intracellular constituents by HPLC. Cells were incubated with 1 mM [^{3}H]AICAR for 1 h after which the intracellular radiolabeled species were assessed by HPLC. As can be seen in Fig. 5A, four peaks were identified: the first coeluted with nonlabeled AICAR, the second coeluted with nonlabeled ZMP, and the two other peaks were assumed to represent ZDP and ZTP. Figure 5B indicates that when cells were exposed to 5-iodotubercidin and [^{3}H]AICAR simultaneously for 1 h, the only peak detected was AICAR, confirming that the other peaks noted in Fig. 5A were derivatives of AICAR. The results of three such experiments are quantified in the legend to Fig. 5. When cells were first incubated with [^{3}H]AICAR for 1 h and then exposed to 5-iodotubercidin for 30 min (Fig. 5C), the ZMP peak was markedly decreased (from 2.13 $\pm$ 0.46 to 0.16 $\pm$ 0.04 mM, ~93%, $p = 0.02$), the ZDP peak was unchanged, and the ZTP peak increased from 1.34 $\pm$ 0.31 to 2.13 $\pm$ 0.32 mM ($p = 0.063$) compared with the levels indicated in Fig. 5A. The increase in ZTP accounted for 40% of the decrease in ZMP that occurred after the 30-min exposure to 5-iodotubercidin.

When cells were exposed to 1 mM [^{3}H]AICAR for 1 h followed by incubation in drug-free buffer for 30 min, the ZMP peak was markedly decreased (from 2.13 $\pm$ 0.46 to 0.16 $\pm$ 0.05 mM, ~93%, $p = 0.045$) (Fig. 5D), a condition in which augmentation of transport by AICAR was reversed (Fig. 4A). Hence, the augmentation of RFC-mediated transport by AICAR and its reversal in AICAR-free buffer correlates with the presence or absence of ZMP within the cells. In another three experiments, the intracellular level of ZMP was assessed by HPLC after a 10-min exposure to 1 mM AICAR, the condition in which transport measurements are made. The intracellular ZMP level achieved within the intracellular water was ~0.77 mM.

Impact of AICAR on the Trans-Stimulation of RFC-Mediated Influx. The unidirectional flux of MTX into cells is augmented when cells are loaded with 5-formyl-THF because of the simultaneous efflux of this folate via RFC, enhancing a rate-limiting step in the transport cycle, a trans-

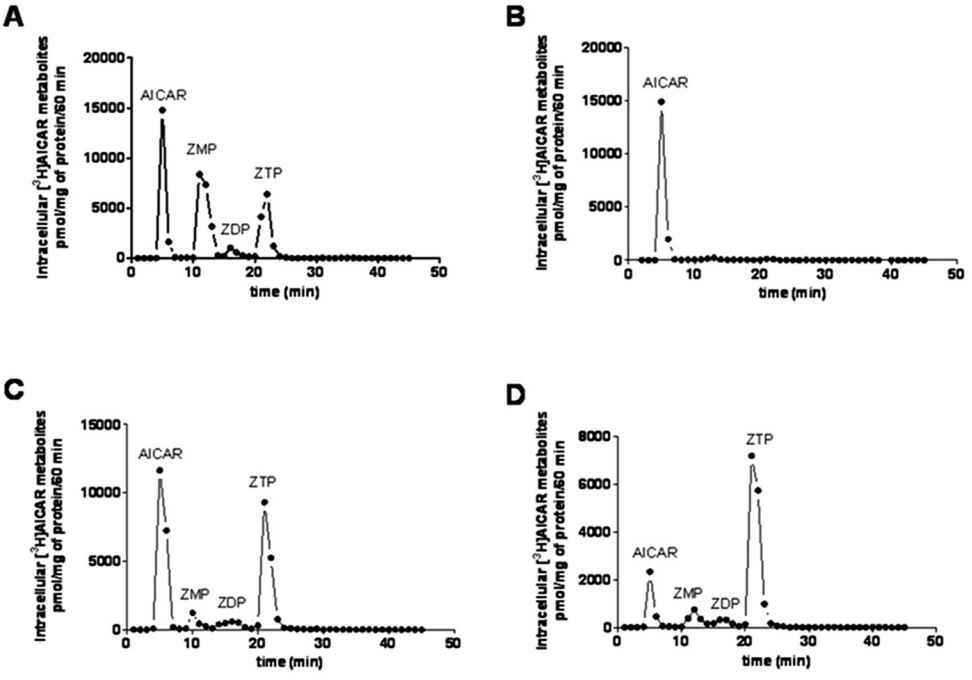

Fig. 5. HPLC analysis of intracellular constituents after incubation of cells with [^{3}H]AICAR. A, HeLa cells were incubated for 1 h with 1 mM [^{3}H]AICAR. B, cells were treated as in A but in the presence of 1 μM 5-iodotubercidin. C, cells were incubated for 1 h with 1 mM [^{3}H]AICAR followed by a 30-min incubation with 1 μM 5-iodotubercidin. D, cells were incubated with 1 mM [^{3}H]AICAR for 1 h and then were incubated for 30 min more in AICAR-free buffer. The chromatograms reflect a representative experiment. The legend quantifies the results from three independent experiments, showing the average value of each intracellular constituent $\pm$ S.E.M.

Intracellular constituents after incubation of cells with [^{3}H]AICAR

mmol/L	A	B	C	D
AICAR	1.62 ± 0.40	2.0 ± 0.40	2.30 ± 0.50	0.58 ± 0.23
ZMP	2.13 ± 0.46	0.03 ± 0.01	0.16 ± 0.04	0.16 ± 0.05
ZDP	0.23 ± 0.05	0.01 ± 0.001	0.16 ± 0.05	0.15 ± 0.02
ZTP	1.34 ± 0.31	0.02 ± 0.01	2.13 ± 0.32	1.95 ± 0.29

stimulation exchange phenomenon (Goldman, 1971). Other studies from this laboratory demonstrated that organic phosphates also use RFC and exchange with folates (Zhao et al., 2001, 2002). If ZMP augments folate influx through an exchange mechanism, then there should be no further enhancement in cells undergoing maximum exchange after loading with high concentrations of a preferred substrate, 5-formyl-THF. Preliminary experiments established that loading cells with 100 μM 5-formyl-THF resulted in maximum trans-stimulation. As indicated in Fig. 6, when cells were preloaded with 100 μM 5-formyl-THF or 1 mM AICAR, each produced comparable augmentation (~60–70%) of [^{3}H]5-methyl-THF influx relative to that in the control cells. However, when cells were loaded with both substrates, there was no further increase in influx compared with that for 5-formyl-THF (p = 0.46) or AICAR (p = 0.35) alone, consistent with effects based on the same mechanism.

Effect of ZMP on RFC-Mediated Influx and Efflux. The data to this point are consistent with an interaction among ZMP, folates, and RFC at the inner cell membrane. According to this paradigm, ZMP synthesized within the cells from exogenous AICAR results in trans-stimulation of folate influx and inhibition of folate efflux, which augments the net level of folates that accumulate within the cells. Thus, ZMP when present extracellularly should inhibit folate influx and when present intracellularly should inhibit folate efflux. This turned out to be the case. Influx of 0.5 μM [^{3}H]MTX was inhibited by the extracellular presence of ZMP with an IC_{50} of ~0.75 mM (Fig. 7, top panel), comparable with the intracellular ZMP level reached after the initial 10-min exposure to this agent (see above). Likewise, as indicated in the bottom panel, when HeLa cells were incubated with 0.5 μM [^{3}H]MTX, in the presence or absence of 1 mM AICAR and then were exposed to 100 μM 5-formyl-THF to block the MTX influx component, the rate constant in the control cells was twice the rate of cells exposed to AICAR ($-3.64 \pm 0.39 \times 10^{-3}$ versus $1.72 \pm 0.23 \times 10^{-3}$ s^{-1}; p = 0.001).

Discussion

AICAR is an exogenous precursor of ZMP, an intermediate in the pathway of purine biosynthesis through its metabolism to IMP mediated by 5-aminoimidazole-4-carboxamide ribonucleoside transformylase (Sabina et al., 1984). Through the formation of ZMP, AICAR leads to the activation of AMP kinase (Davies et al., 1995; Corradetti and Guan, 2006). A variety of pharmacologic applications of AICAR have been explored: 1) postmyocardial ischemia cardioprotection based upon its salutary effect on purine synthesis (Swain et al., 1982; Mitsos et al., 1985) or 2) as a chemotherapeutic agent alone (Rattan et al., 2005; Van Den Neste et al., 2010; Tang et al., 2011) or in combination with ionizing radiation or cytotoxic agents such as MTX (Beckers et al., 2006; Isebaert et al., 2011). AICAR has antiproliferative and proapoptotic activity in aneuploid cells as a result of both suppression of mTOR signaling and mTOR independent mechanisms, in one case resulting from activation of p53 (Rattan et al., 2005; Swinnen et al., 2005; Tang et al., 2011).

In this report, we expand the understanding of the mechanistic basis for the previously reported impact of AICAR on folate and antifolate uptake by kinetic analyses and assessment of AICAR metabolism within cells (McGuire et al., 2006). Augmentation of folate transport in HeLa cells by AICAR is due to the following: 1) AICAR transport into cells, 2) the formation of ZMP from AICAR within cells, and 3) inhibition by ZMP of folate efflux and trans-stimulation of folate influx that together produce a substantial augmentation of net folate uptake. Augmentation of transport by this mechanism was observed for MTX and the reduced folates, 5-formyl-THF and 5-methyl-THF. The use of HeLa cell lines that express either PCFT or RFC confirmed that this phenomenon is due solely to an interaction among ZMP, folates, and RFC (Fig. 8). The rapid metabolism of AICAR to ZMP as assessed by HPLC is consistent with what has been observed by other investigators (Thomas et al., 1981).

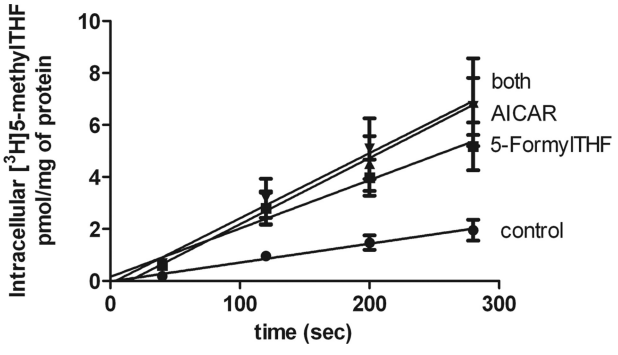

Fig. 6. Impact of AICAR on trans-stimulation mediated by 5-formyl-THF. HeLa cells were loaded for 20 min with 1 mM AICAR, 100 μM 5-formyl-THF, or both. The cells were then washed in 0°C HBS after which influx of 0.5 μM [^{3}H]5-methyl-THF was assessed. Data are the mean ± S.E.M. from four independent experiments.

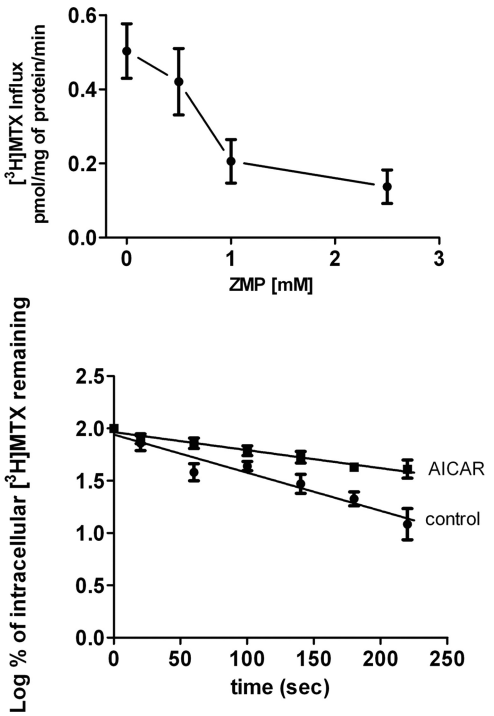

Fig. 7. Inhibitory effect of ZMP on [^{3}H]MTX influx and efflux. Top panel, influx of 0.5 μM [^{3}H]MTX was assessed in HeLa cells in the absence or presence of nonlabeled ZMP at the indicated concentrations. Bottom panel, impact of AICAR on [^{3}H]MTX efflux. HeLa cells were incubated for 30 min with 0.5 μM [^{3}H]MTX in the presence or absence of 1 mM AICAR after which 100 μM 5-formyl-THF was added to block [^{3}H]MTX influx, and the decline of intracellular [^{3}H]MTX was monitored. Data are the mean ± S.E.M. from six independent experiments.

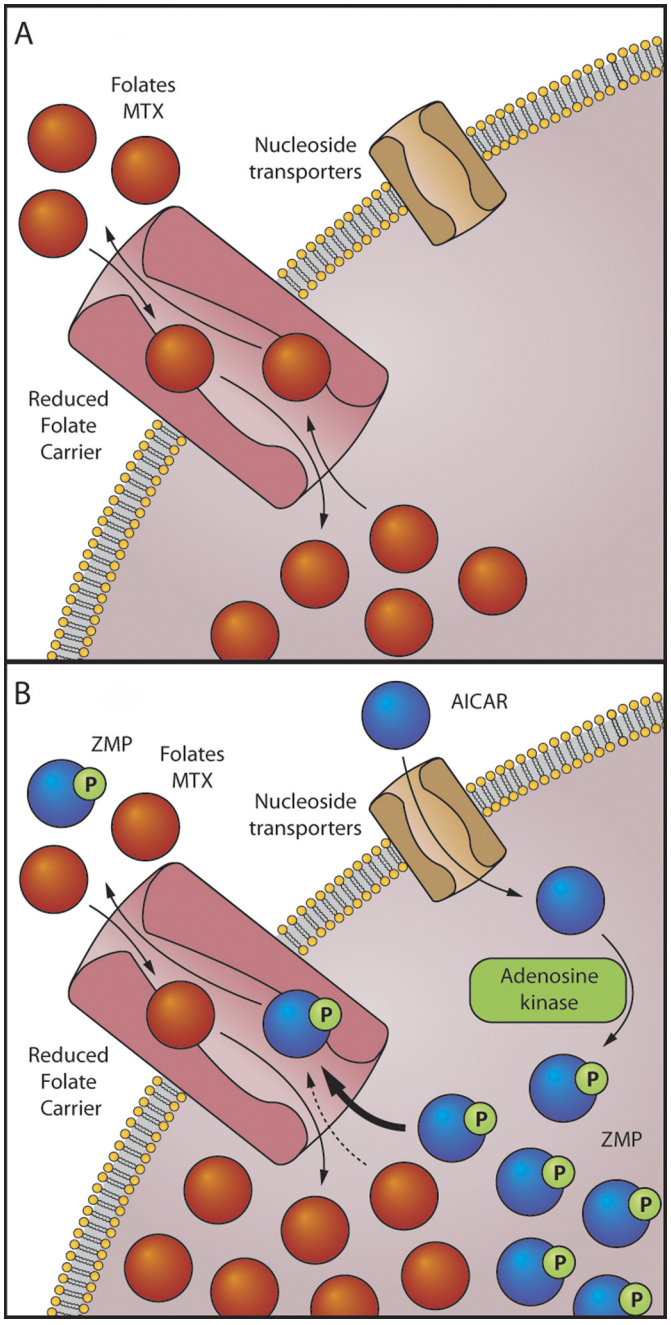

Fig. 8. Model for a ZMP-folate antiport mechanism mediated by RFC. A, under physiological conditions intracellular ZMP levels are negligible. RFC mediates the bidirectional fluxes of folates across the cell membrane. B, after entering the cells via nucleoside transporters, AICAR is rapidly converted to ZMP by adenosine kinase. Intracellular ZMP competes with intracellular folates at the inner cell membrane for export via RFC, which results in inhibition of folate efflux and trans-stimulation of folate influx, leading to augmentation of the net level of folate accumulation within the cells.

Of interest were the observations that after cells had accumulated ZMP, and AICAR was removed or 5-iodotubercidin was added, the intracellular ZMP level rapidly decreased and the augmentation of folate transport was reversed. Hence, continued synthesis of ZMP is required to sustain intracellular ZMP levels and the augmentation of RFC-mediated transport. Neither AICAR itself nor ZTP within the cells resulted in augmentation of folate transport. The basis for the rapid decrease of intracellular ZMP under these conditions is due in part to the conversion of ZMP to ZTP and to export mediated by RFC. It is also possible that a component of the decrease in cell ZMP was due to rapid hydrolysis back to the base.

This interaction between ZMP and folates at the level of a common carrier is a classic exchange reaction in which the transmembrane gradient for one substrate drives the uphill transport of another. Most uphill systems for members of the SLC superfamily of solute transport carriers derive their energy through a cotransport with either a sodium ion or a proton (Forrest and Rudnick, 2009). In the case of PCFT, folates and protons are cotransported by this mechanism, and the flow of protons down the transmembrane proton gradient into cells provides the energy that drives the uphill transport of folates into cells (Qiu et al., 2006; Unal et al., 2009). On the other hand, RFC is an organic phosphate antiporter. In this case, the uphill flow of folates into cells via RFC is due to the inhibition of folate export by organic phosphates as these molecules flow out of cells down their electrochemical potential gradient via RFC (Zhao et al., 2009, 2011).

In the case of AICAR, this molecule enters cells by a nucleoside transporter (Gadalla et al., 2004). Folates do not use this transporter and AICAR does not use or inhibit RFC. Hence, both substrates enter the cells by their respective mechanisms. Once in the cell, however, AICAR is converted to ZMP, which is a substrate for RFC. Inhibition of RFC-mediated folate export under conditions in which the extracellular ZMP concentration is trivial (in which there is a very high transmembrane ZMP gradient) results in uphill folate transport in the cells. In the case of MTX, which is not metabolized over the interval of these experiments, there is a marked increase in the transmembrane electrochemical potential difference across the cell membrane in the presence of AICAR. Uphill transport of MTX must be accounted for, energetically, by the export of ZMP via RFC down its electrochemical potential gradient, a transduction mediated by the same carrier. This is similar to what was observed for the interaction between thiamine and MTX. Thiamine enters cells via SLC19A2 or SLC19A3, neither of which transports folates. Once in the cell, thiamine is metabolized to its mono- and diphosphate derivatives, which are substrates for RFC and are exported by this mechanism (Zhao et al., 2001, 2002).

There are some differences between these findings in HeLa cells and what was reported earlier in studies with CCRF-CEM human T leukemia cells (McGuire et al., 2006). For instance, stimulation of MTX influx by AICAR was delayed even when cells were pretreated with this agent, becoming instantaneous when cells were pretreated with trimetrexate, a lipophilic DHFR inhibitor. Likewise, augmentation of net 5-formyl-THF uptake by AICAR only occurred if cells were pretreated with trimetrexate, leading the authors to suggest that inhibition of tetrahydrofolate generation is a *conditio sine qua non* for AICAR potentiation (McGuire et al., 2006). However, in the current study, augmentation of 5-formyl-THF and of 5-methyl-THF and MTX, initial rates occurred without any prior perturbation of DHFR activity. The earlier conclusion that this phenomenon was RFC-specific was based on the observation that it did not occur in cells that lack RFC. However, because there was no way for folates to enter CCRF-CEM cells that lack RFC, it was not possible to

evaluate a possible role for other transporter(s) that might act on the disposition of intracellular folates. This possibility was excluded by the observation that AICAR potentiation did not occur when folates accumulated in HeLa cells that selectively express only PCFT.

This interaction between ZMP and folates at the level of RFC could have pharmacological ramifications for antifolates currently in clinical use (Goldman et al., 2010). For instance, recent studies indicate that high levels of ZMP build up in cells after exposure to pemetrexed as a consequence of the inhibition of AICART by pemetrexed polyglutamate derivatives. This results in activation of AMP kinase and consequent inhibition of mTOR (Racanelli et al., 2009). The current study raises the possibility of another consequence of the buildup of ZMP in cells by pemetrexed, the augmentation of the RFC-mediated transport of this agent.

Acknowledgments

We thank Dr. Lorenzo Agoni for providing Fig. 8 and Dr. Andong Qiu for the development of the HeLa R1-PCFT cell line during his postdoctoral fellowship in this laboratory.

Authorship Contributions

Participated in research design: Visentin, Zhao, and Goldman.
Conducted experiments: Visentin.
Performed data analysis: Visentin.
Wrote or contributed to the writing of the manuscript: Visentin and Goldman.

References

Assaraf YG (2006) The role of multidrug resistance efflux transporters in antifolate resistance and folate homeostasis. *Drug Resist Updat* **9:**227–246.
Beckers A, Organe S, Timmermans L, Vanderhoydonc F, Deboel L, Derua R, Waelkens E, Brusselmans K, Verhoeven G, and Swinnen JV (2006) Methotrexate enhances the antianabolic and antiproliferative effects of 5-aminoimidazole-4-carboxamide riboside. *Mol Cancer Ther* **5:**2211–2217.
Corradetti MN and Guan KL (2006) Upstream of the mammalian target of rapamycin: do all roads pass through mTOR? *Oncogene* **25:**6347–6360.
Davies SP, Helps NR, Cohen PT, and Hardie DG (1995) 5′-AMP inhibits dephosphorylation, as well as promoting phosphorylation, of the AMP-activated protein kinase. Studies using bacterially expressed human protein phosphatase-2Cα and native bovine protein phosphatase-2AC. *FEBS Lett* **377:**421–425.
Diop-Bove NK, Wu J, Zhao R, Locker J, and Goldman ID (2009) Hypermethylation of the human proton-coupled folate transporter (SLC46A1) minimal transcriptional regulatory region in an antifolate-resistant HeLa cell line. *Mol Cancer Ther* **8:**2424–2431.
Forrest LR and Rudnick G (2009) The rocking bundle: a mechanism for ion-coupled solute flux by symmetrical transporters. *Physiology* (*Bethesda*) **24:**377–386.
Gadalla AE, Pearson T, Currie AJ, Dale N, Hawley SA, Sheehan M, Hirst W, Michel AD, Randall A, Hardie DG, et al. (2004) AICA riboside both activates AMP-activated protein kinase and competes with adenosine for the nucleoside transporter in the CA1 region of the rat hippocampus. *J Neurochem* **88:**1272–1282.
Goldman ID (1971) A model system for the study of heteroexchange diffusion: methotrexate-folate interactions in L1210 leukemia and Ehrlich ascites tumor cells. *Biochim Biophys Acta* **233:**624–634.
Goldman ID, Chattopadhyay S, Zhao R, and Moran R (2010) The antifolates: evolution, new agents in the clinic, and how targeting delivery via specific membrane transporters is driving the development of a next generation of folate analogs. *Curr Opin Investig Drugs* **11:**1409–1423.
Isebaert SF, Swinnen JV, McBride WH, Begg AC, and Haustermans KM (2011) 5-Aminoimidazole-4-carboxamide riboside enhances effect of ionizing radiation in PC3 prostate cancer cells. *Int J Radiat Oncol Biol Phys* **81:**1515–1523.
Kamen BA and Smith AK (2004) A review of folate receptor alpha cycling and 5-methyltetrahydrofolate accumulation with an emphasis on cell models in vitro. *Adv Drug Deliv Rev* **56:**1085–1097.
Matherly LH and Hou Z (2008) Structure and function of the reduced folate carrier a paradigm of a major facilitator superfamily mammalian nutrient transporter. *Vitam Horm* **79:**145–184.
McGuire JJ, Haile WH, and Yeh CC (2006) 5-Amino-4-Imidazolecarboxamide riboside potentiates both transport of reduced folates and antifolates by the human reduced folate carrier and their subsequent metabolism. *Cancer Res* **66:**3836–3844.
Mitsos SE, Jolly SR, and Lucchesi BR (1985) Protective effects of AICAriboside in the globally ischemic isolated cat heart. *Pharmacology* **31:**121–131.
Parkinson FE and Geiger JD (1996) Effects of iodotubercidin on adenosine kinase activity and nucleoside transport in DDT1 MF-2 smooth muscle cells. *J Pharmacol Exp Ther* **277:**1397–1401.
Qiu A, Jansen M, Sakaris A, Min SH, Chattopadhyay S, Tsai E, Sandoval C, Zhao R, Akabas MH, and Goldman ID (2006) Identification of an intestinal folate transporter and the molecular basis for hereditary folate malabsorption. *Cell* **127:**917–928.
Racanelli AC, Rothbart SB, Heyer CL, and Moran RG (2009) Therapeutics by cytotoxic metabolite accumulation: pemetrexed causes ZMP accumulation, AMPK activation, and mammalian target of rapamycin inhibition. *Cancer Res* **69:**5467–5474.
Rattan R, Giri S, Singh AK, and Singh I (2005) 5-Aminoimidazole-4-carboxamide-1-β-D-ribofuranoside inhibits cancer cell proliferation in vitro and in vivo via AMP-activated protein kinase. *J Biol Chem* **280:**39582–39593.
Sabina RL, Holmes EW, and Becker MA (1984) The enzymatic synthesis of 5-amino-4-imidazolecarboxamide riboside triphosphate (ZTP). *Science* **223:**1193–1195.
Sharif KA and Goldman ID (2000) Rapid determination of membrane transport parameters in adherent cells. *Biotechniques* **28:**926–928, 930, 932.
Swain JL, Hines JJ, Sabina RL, and Holmes EW (1982) Accelerated repletion of ATP and GTP pools in postischemic canine myocardium using a precursor of purine de novo synthesis. *Circ Res* **51:**102–105.
Swinnen JV, Beckers A, Brusselmans K, Organe S, Segers J, Timmermans L, Vanderhoydonc F, Deboel L, Derua R, Waelkens E, et al. (2005) Mimicry of a cellular low energy status blocks tumor cell anabolism and suppresses the malignant phenotype. *Cancer Res* **65:**2441–2448.
Tang YC, Williams BR, Siegel JJ, and Amon A (2011) Identification of aneuploidy-selective antiproliferation compounds. *Cell* **144:**499–512.
Thomas CB, Meade JC, and Holmes EW (1981) Aminoimidazole carboxamide ribonucleoside toxicity: a model for study of pyrimidine starvation. *J Cell Physiol* **107:**335–344.
Unal ES, Zhao R, and Goldman ID (2009) Role of the glutamate 185 residue in proton translocation mediated by the proton-coupled folate transporter SLC46A1. *Am J Physiol Cell Physiol* **297:**C66–C74.
Van Den Neste E, Van den Berghe G, and Bontemps F (2010) AICA-riboside (acadesine), an activator of AMP-activated protein kinase with potential for application in hematologic malignancies. *Expert Opin Investig Drugs* **19:**571–578.
Zhao R, Babani S, Gao F, Liu L, and Goldman ID (2000) The mechanism of transport of the multitargeted antifolate (MTA) and its cross-resistance pattern in cells with markedly impaired transport of methotrexate. *Clin Cancer Res* **6:**3687–3695.
Zhao R, Diop-Bove N, Visentin M, and Goldman ID (2011) Mechanisms of membrane transport of folates into cells and across epithelia. *Annu Rev Nutr* **31:**177–201.
Zhao R, Gao F, and Goldman ID (2002) Reduced folate carrier transports thiamine monophosphate: an alternative route for thiamine delivery into mammalian cells. *Am J Physiol Cell Physiol* **282:**C1512–C1517.
Zhao R, Gao F, Hanscom M, and Goldman ID (2004a) A prominent low-pH methotrexate transport activity in human solid tumors: contribution to the preservation of methotrexate pharmacologic activity in HeLa cells lacking the reduced folate carrier. *Clin Cancer Res* **10:**718–727.
Zhao R, Gao F, Wang Y, Diaz GA, Gelb BD, and Goldman ID (2001) Impact of the reduced folate carrier on the accumulation of active thiamin metabolites in murine leukemia cells. *J Biol Chem* **276:**1114–1118.
Zhao R, Hanscom M, Chattopadhyay S, and Goldman ID (2004b) Selective preservation of pemetrexed pharmacological activity in HeLa cells lacking the reduced folate carrier: association with the presence of a secondary transport pathway. *Cancer Res* **64:**3313–3319.
Zhao R, Matherly LH, and Goldman ID (2009) Membrane transporters and folate homeostasis: intestinal absorption and transport into systemic compartments and tissues. *Expert Rev Mol Med* **11:**e4.
Zhao R, Qiu A, Tsai E, Jansen M, Akabas MH, and Goldman ID (2008) The proton-coupled folate transporter: impact on pemetrexed transport and on antifolates activities compared with the reduced folate carrier. *Mol Pharmacol* **74:**854–862.
Zhao R, Seither R, Brigle KE, Sharina IG, Wang PJ, and Goldman ID (1997) Impact of overexpression of the reduced folate carrier (RFC1), an anion exchanger, on concentrative transport in murine L1210 leukemia cells. *J Biol Chem* **272:**21207–21212.

Address correspondence to: I. David Goldman, Albert Einstein Cancer Center, Chanin 2, 1300 Morris Park Ave., Bronx, NY 10461. E-mail: i.david.goldman@einstein.yu.edu